Kinetics for Hybridization of Peptide Nucleic Acids (PNA) with DNA and RNA Studied with the BIAcore Technique†

Kristine Kilså Jensen,‡,§ Henrik Ørum,|| Peter E. Nielsen,‡ and Bengt Nordén*,§

Center for Biomolecular Recognition, Department of Medical Biochemistry and Genetics, The Panum Institute, Blegdamsvej 3c, DK-2200 Copenhagen N, Denmark, PNA Diagnostics A/S, Rønnegade 2, DK-2100 Copenhagen Ø, Denmark, and Department of Physical Chemistry, Chalmers University of Technology, S-412 96 Gothenburg, Sweden

Received November 4, 1996; Revised Manuscript Received February 18, 1997⊗

ABSTRACT: The binding of a mixed-sequence pentadecamer PNA (peptide nucleic acid) containing all four nucleobases to the fully complementary as well as various singly mismatched RNA and DNA oligonucleotides has been systematically investigated using thermal denaturation and BIAcore surface-interaction techniques. The rate constants for association (k_a) and dissociation (k_d) of the duplex formation as well as the thermal stability (melting temperature, T_m) of the duplexes have been determined. Upon binding to PNA tethered via a biotin-linker to streptavidin at the dextran/gold surface, DNA and RNA sequences containing single mismatches at various positions in the center resulted in increased dissociation and decreased association rate constants. T_m values for PNA•RNA duplexes are on average 4 °C higher than for PNA•DNA duplexes and follow quantitatively the same variation with mismatches as do the PNA•DNA duplexes. Also a faster k_a and a slower k_d are found for PNA•RNA duplexes compared to the PNA•DNA duplexes. An overall fair correlation between T_m, k_a, and k_d is found for a series of PNA•DNA and PNA•RNA duplexes although the determination of k_a seemed to be prone to artifacts of the method and was not considered capable of providing absolute values representing the association rate constant in bulk solution.

Peptide nucleic acids (PNA) have attracted wide attention in the context of development of antisense and antigene therapeutic agents (Nielsen *et al.*, 1991, 1994a,b; Hanvey *et al.*, 1992; Egholm *et al.*, 1993; Demidov *et al.*, 1994; Bonham *et al.*, 1995; Knudsen *et al.*, 1996). Also a variety of applications within molecular biology and diagnostics have emerged from PNA chemistry (Demidov *et al.*, 1993, 1995; Ørum *et al.*, 1993, 1995; Nielsen & Ørum, 1995; Veselkov *et al.*, 1996). PNA can be regarded a DNA mimic in which the normal DNA bases are attached to an achiral, nonionic pseudopeptide backbone composed of *N*-(2-aminoethyl)-glycine units (Figure 1; Nielsen *et al.*, 1991; Dueholm *et al.*, 1994; Christensen *et al.*, 1995). This structure appears to give very favorable DNA and RNA hybridization properties: thermal stability (T_m) measurements suggest that PNA•DNA duplexes at physiological salt conditions are considerably more stable than the corresponding DNA•DNA duplexes without sacrificing sequence discrimination (Egholm *et al.*, 1993). The finding that PNA also binds very strongly and sequence specifically to RNA is of interest for potential antisense applications.

So far no systematic kinetic or thermodynamic studies of the sequence discrimination of PNA•RNA or PNA•DNA hybridization reactions have been reported although such data would be very important for the evaluation and improvement of antisense reagents and of diagnostic probes based on PNA. We here present the first systematic study of PNA•RNA sequence discrimination (thermal stabilities, T_m) using a pentadecamer mixed-sequence PNA containing all four nucleobases interacting with the fully complementary as well as various singly mismatched oligonucleotides. Furthermore, the kinetics of the association and dissociation reactions of PNA•DNA, PNA•RNA, DNA•DNA, and PNA•PNA hybridization was determined using a BIAcore surface-plasmon resonance detection equipment.

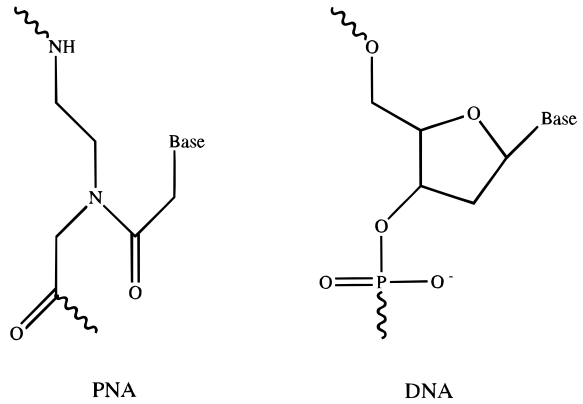

FIGURE 1: Chemical structure of a PNA monomer as compared to a DNA nucleotide.

MATERIALS AND METHODS

Chemicals. The synthesis of PNA was carried out as described using Boc-PNA-monomers obtained from Perseptive Biosystems (Christensen *et al.*, 1995). Biotin was coupled to the amino terminal using biotin-NHS ester. DNA oligonucleotides were synthesized using the standard solid support phosphoramidite technique. RNA oligonucleotides

† This project has been supported by the Danish National Research Foundation and the Swedish Natural Science Research Council.

* To whom correspondence should be addressed.
‡ The Panum Institute.
§ Chalmers University of Technology.
|| PNA Diagnostics A/S.

⊗ Abstract published in *Advance ACS Abstracts,* April 1, 1997.

S0006-2960(96)02752-3 CCC: $14.00 © 1997 American Chemical Society

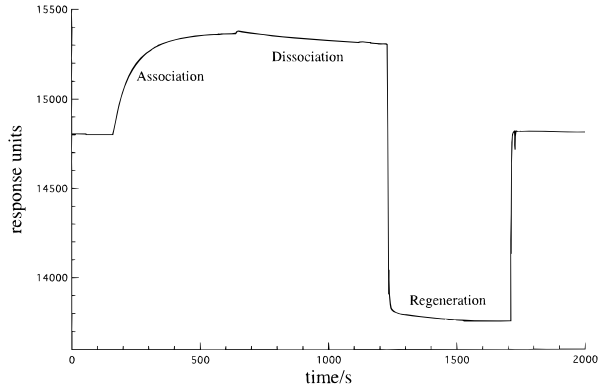

FIGURE 2: Typical response features ("sensorgrams") as measured by the BIAcore technique. The figure refers to a DNA•DNA hybridization (1.5 μM of the fully complementary associating strand), dissociation by purging buffer (PBS) and regeneration by purging 10 mM HCl over the dextran/streptavidin surface.

were purchased from DNA Technology Aps (Århus, Denmark). All other chemicals were of p.a. grade and used as obtained without further purification.

Kinetic Measurements. Kinetic parameters were assessed using a BIAcore (Biomolecular Interaction Analysis) equipment with a SensorChip SA5 from Pharmacia. The central part of this equipment is the sensor-chip consisting of a gold surface covered with a layer of dextran which in our case contained streptavidin chemically coupled to the dextran. When not otherwise stated, a biotin-PNA strand [biotin-$(eg1)_3$-TGT ACG TCA CAA CTA-NH_2 (N- to C-terminal); eg1 = 8-amino-3,6-dioxyoctanoic acid] (Egholm *et al.*, 1995) was immobilized to the streptavidin chip.

The response signal of the BIAcore apparatus is proportional to the change in the refractive index at the surface and is generally assumed to be proportional to the mass of substance bound to the chip (Jönsson, 1991; Fägerstam & Karlsson, 1993; Malmqvist, 1993; Malmqvist & Granzow, 1994). By measuring the amount of bound substance as a function of time when a solution containing the complementary strands passes over the chip surface, the kinetics of association to the immobilized PNA were studied. The dissociation kinetics were correspondingly monitored by detecting the time dependence of the mass decrease as the surface was subsequently washed with buffer. The PNA surface could thereafter be regenerated by washing with strong acid, HCl (removing of all the remaining hybridized products) (Fägerstam & Karlsson, 1993; Malmqvist, 1993), thereby enabling consecutive studies with the same immobilized PNA (Figure 2).

The association as well as dissociation kinetics of four types of fully complementary pentadecamer duplexes, PNA•DNA, PNA•RNA, PNA•PNA, and DNA•DNA, were studied. For the PNA•DNA, PNA•RNA, and DNA•DNA complexes, the 12 possible DNA (RNA) combinations having 1 mismatch in 1 of the 4 central base positions were studied as well. All investigated duplexes had "antiparallel" orientations of the strands, i.e., 5′-3′•3′-5′ for DNA•DNA, N-C•3′-5′ for PNA•DNA and PNA•RNA, and N-C•C-N for PNA•PNA.

For the analysis of the hybridization kinetics, a two-state model, A + B $\rightleftharpoons$ AB, was assumed. The dissociation kinetics (Figure 3), obtained from the dissociation part of the sensorgram, were found to be essentially independent of concentration for all duplexes and were analyzed according to

$$[\mathrm{AB}] = [\mathrm{AB}]_0 e^{-k_d(t-t_0)} \quad (1)$$

where $[AB]_0$ is the duplex concentration at time t_0 and k_d the dissociation rate constant. The association kinetics (Figure 3) were analyzed with respect to the concentration dependence of the association rate by varying the concentration of the agent, A, in the mobile phase:

$$[\mathrm{AB}] = \frac{k_a[\mathrm{A}][\mathrm{B}]_0}{k_a[\mathrm{A}] + k_d}[1 - e^{-(k_a[\mathrm{A}]+k_d)t}] \quad (2)$$

By setting $k_a[A] + k_d = k_s$ and measuring k_s at different concentrations of A, the association rate constant was obtained as the slope of a k_s *versus* [A] plot (Fägerstam & Karlsson, 1993; Malmqvist, 1993; O'Shannessy *et al.*, 1993).

All kinetic experiments were performed in a PBS buffer (150 mM NaCl aqueous solution containing 0.1 mM EDTA and 20 mM sodium phosphate adjusted to pH 7.0) which for RNA hybridizations was treated with diethyl pyrocarbonate. The experiments were performed at 35 °C for all systems except for the DNA•DNA hybridizations, which were carried out at 20 °C. To immobilize the biotinylated PNA (DNA) strand to the streptavidin on the chip surface, biotin-labeled PNA (N-terminal) or DNA (5′-end) was dissolved in degassed PBS buffer at a concentration of 2 μM. The solution (40 μL) was injected with a flow rate of 5 μL/min, and the immobilization was followed in the corresponding sensorgram as a function of time. Typically 80 pmol of PNA (or DNA) was bound to the streptavidin in the flow cell.

Complementary or mismatch strands were dissolved in PBS buffer at appropriate concentrations (0.05−60 μM). A volume of 40 μL (5 μL/min) was injected to measure the association kinetics, and immediately thereafter the dissociation was followed by purging PBS buffer through the system. After approximately 500 s of buffer wash, the immobilized single-strand PNA (DNA) surface was regenerated with 40 μL of 10 mM HCl (5 μL/min) for the PNA•DNA, PNA•PNA, and DNA•DNA duplexes and 40 μL of 100 mM HCl (5 μL/min) for the PNA•RNA duplexes.

Melting Temperatures. Melting temperatures, T_m, were determined in 100 mM NaCl, 0.1 mM EDTA, and 10 mM sodium phosphate, adjusted to pH 7.0, by measuring the hypochromicity at 260 nm as a function of temperature on a Gilford Response UV−Vis spectrophotometer, recording the absorbance at 260 nm and increasing the temperature in steps of 0.5 °C/min from 15 to 90 °C. The two strands were mixed in equimolar amounts to give a total absorbance at high temperature around $A_{260} = 0.5$. Annealing was performed by heating the sample to 90 °C, a temperature it was kept at for 5 min, followed by cooling to room temperature during 30 min, keeping the samples at 5 °C for at least 45 min.

The melting curves represent at all temperatures the equilibrium between the duplex and the two single strands. Combining the relation

$$\Delta G^\circ = \Delta H^\circ - T\Delta S^\circ = -RT \ln K_D \quad (3)$$

with the expression for K_D

$$K_D = \frac{c_T}{2}\frac{(1-\alpha)^2}{\alpha} \quad (4)$$

gives at $T = T_m$ ($\alpha = {}^1/_2$):

$$\frac{1}{T_m} = \frac{\Delta S^\circ + R \ln 4}{\Delta H^\circ} - \frac{R}{\Delta H^\circ} \ln c_T \qquad (5)$$

where R is the gas constant, c_T is the total strand concentration, and α is the fraction of the duplex (Marky & Breslauer, 1987). Thus, analyzing the melting curves with different strand concentration yields the enthalpy and entropy for the reaction. Thereby K_D can be calculated using eq 3 at any temperature. From these relationships, a correlation of K_D with T_m is expected.

RESULTS AND DISCUSSION

Our results are interesting from several perspectives. Very few reports have yet been published on nucleic acid interactions using the BIAcore technique (Wood, 1993; Nilsson *et al.*, 1995; Gotoh *et al.*, 1996). Our results also represent the first systematic study of effects of mismatches of a nucleic acid mimic on the association and dissociation kinetics using the very simple approach of having one strand immobilized to a surface and monitoring the extra association to the surface. Clearly, this technique is sensitive and reproducible enough not only to discriminate the gross differences previously observed in terms of variations in thermal stability between the different hybrid combinations PNA•DNA, PNA•RNA, DNA•DNA, and PNA•PNA, but also to pick up more subtle differences which may be important for understanding of the mechanism of hybridization and of recognition of a fully complementary sequence in gene diagnostic and therapeutic contexts.

The kinetics of association of the immobilized pentadecamer PNA, biotin-(eg1)$_3$-TGT ACG TCA CAA CTA-NH_2, to a complementary strand of DNA, RNA, or PNA could be successfully monitored with high fidelity as trajectories over minutes using the BIAcore technology. In contrast, the DNA•DNA hybridization was found to be more difficult to numerically reproduce, although the gross trend along the mismatch series was reproducible (see below).

Figure 3 shows typical BIAcore trajectories of PNA•DNA hybridization run at different concentrations of the complementary DNA strand free in solution. For all investigated duplexes, the hybridization experiments were made with at least four different concentrations of the associating strand. As expected, the dissociation kinetics showed no significant dependence of concentration, while the association rate increased with the concentration of the incoming strand. The dissociation rate constants reported here are the averages of k_d values determined at the different concentrations of the incoming strand. In the association part of the sensorgram, both association and dissociation contribute to the shape of the trajectory. An approximately linear correlation of the observed rate constant with concentration of associating strand was found. Assuming a two-state model, A + B $\rightleftharpoons$ AB, the observed rate constant, k_s, will be given as $k_s = k_a[A] + k_d$, with A denoting the strand in the mobile phase. Thus, k_a is obtained as the slope of a k_s *versus* [A] plot. It should be noted that the values obtained for the association rate constants, and thereby the equilibrium constant K_D ($= k_d/k_a$), refer to the specific conditions of the dextran surface and, therefore, cannot be directly applied to bulk solution. In addition to the fully complementary strand, all possible combinations of single mismatches introduced among the central four base pairs were investigated for all systems

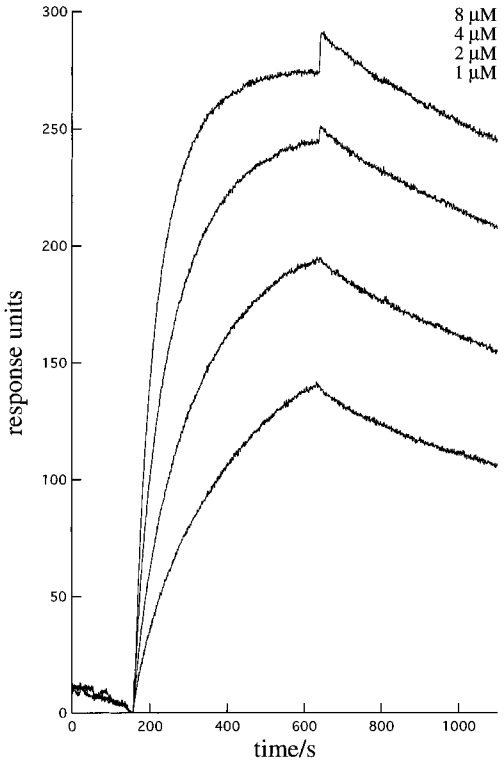

FIGURE 3: PNA•DNA sensorgrams (fully complementary duplex) with varying concentrations of the associating DNA strand: 8 μM, 4 μM, 2 μM, and 1 μM, respectively, from top to bottom.

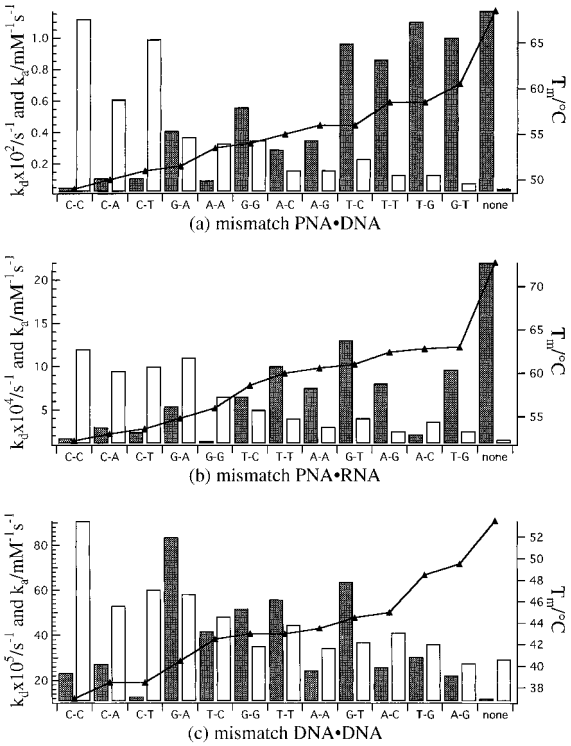

FIGURE 4: Correlation of T_m (▲) with k_a (shaded bars) and k_d (unfilled bars) for PNA•DNA (a), PNA•RNA (b), and DNA•DNA (c) duplexes at 0.1 M ionic strength. PNA•DNA and PNA•RNA refer to 35 °C and DNA•DNA to 20 °C. Note that k_a and k_d are plotted on the same axis.

except PNA•PNA. The collected results with mismatches for PNA•DNA, PNA•RNA, and DNA•DNA are presented in Figure 4a−c and Tables 1 and 2.

The melting temperatures for PNA•RNA duplexes are on average 4 °C higher than those of the corresponding PNA•DNA duplexes. For this series, the PNA•RNA data

Table 1: Effects of Mismatches (Indicated by Boldface Letters) on Melting Temperature (T_m), Dissociation (k_d) and Association (k_a) Rate Constants, and (Calculated) Dissociation Equilibrium Constants (K_D) for PNA•DNA and PNA•RNA Duplexes at 35 °C

sequence (5′-3′) of associating strand[a]	mismatch base pair[a]	T_m DNA (°C)	k_d DNA ($\times 10^{-3}$ s^{-1})[b]	k_a DNA (mM^{-1} s^{-1})[b]	K_D DNA ($\times 10^{-5}$ M)	T_m RNA (°C)	k_d RNA ($\times 10^{-3}$ s^{-1})[b]	k_a RNA (mM^{-1} s^{-1})[b]	K_D RNA ($\times 10^{-8}$ M)
TAG TTG TGA CGT ACA	none	68.5	0.41	1.17	0.035	72.8	0.15	22	0.68
TAG TTG **C**GA CGT ACA	A-C	55.0	1.6	0.29	0.55	62.8	0.36	2.1	17
TAG TTG **G**GA CGT ACA	A-G	56.0	1.6	0.35	0.46	62.4	0.25	8.0	3.1
TAG TTG **A**GA CGT ACA	A-A	53.5	3.3	0.095	3.5	60.6	0.30	7.5	4.0
TAG TTG T**C**A CGT ACA	C-C	49.0	11.2	0.05	22	52.2	1.2	1.7	71
TAG TTG T**T**A CGT ACA	C-T	51.0	9.9	0.11	9.0	53.6	1.0	2.4	42
TAG TTG T**A**A CGT ACA	C-A	50.0	6.1	0.11	5.5	53.0	0.95	3.0	32
TAG TTG TG**T** CGT ACA	T-T	58.5	1.3	0.86	0.15	60.0	0.40	10	4.0
TAG TTG TG**C** CGT ACA	T-C	56.0	2.3	0.96	0.24	58.6	0.50	6.5	7.7
TAG TTG TG**G** CGT ACA	T-G	58.5	1.3	1.1	0.12	63.0	0.25	9.6	2.6
TAG TTG TGA **G**GT ACA	G-G	54.0	3.5	0.56	0.63	56.0	0.65	1.4	46
TAG TTG TGA **T**GT ACA	G-T	60.5	0.76	1.0	0.76	61.0	0.40	13	3.1
TAG TTG TGA **A**GT ACA	G-A	51.5	3.7	0.41	0.90	54.8	1.1	5.4	20

[a] In the RNA strands, thymine is substituted with uracil. [b] Typical error levels for the k_d and k_a values are ±15%.

Table 2: Effects of Mismatches (Indicated by Boldface Letters) on Melting Temperature (T_m), Dissociation (k_d) and Association (k_a) Rate Constants, and (Calculated) Dissociation Equilibrium Constants (K_D) for DNA•DNA Duplexes at 20 °C

sequence (5′-3′) of associating strand	mismatch base pair	T_m (°C)	k_d ($\times 10^{-3}$ s^{-1})[a]	k_a (mM^{-1} s^{-1})[a,b]	K_D ($\times 10^{-8}$ M)[b]
TAG TTG TGA CGT ACA	none	53.5	0.29	12	2.5
TAG TTG **C**GA CGT ACA	A-C	45.0	0.41	26	1.6
TAG TTG **G**GA CGT ACA	A-G	49.5	0.28	22	1.3
TAG TTG **A**GA CGT ACA	A-A	43.5	0.34	24	1.4
TAG TTG T**C**A CGT ACA	C-C	37.0	0.91	23	3.9
TAG TTG T**T**A CGT ACA	C-T	38.5	0.53	27	2.0
TAG TTG T**A**A CGT ACA	C-A	38.5	0.60	13	4.7
TAG TTG TG**T** CGT ACA	T-T	43.0	0.35	52	0.68
TAG TTG TG**C** CGT ACA	T-C	42.5	0.48	42	1.2
TAG TTG TG**G** CGT ACA	T-G	48.5	0.36	30	1.2
TAG TTG TGA **G**GT ACA	G-G	43.0	0.45	56	0.80
TAG TTG TGA **T**GT ACA	G-T	44.5	0.37	64	0.58
TAG TTG TGA **A**GT ACA	G-A	40.5	0.58	84	0.70

[a] Typical error levels for the k_d values are ±15% and for the k_a values ±25%. [b] Ambiguities, see text.

Table 3: Comparison of Melting Temperatures (T_m), Dissociation (k_d) and Association (k_a) Rate Constants, and Dissociation Equilibrium Constants (K_D) for the Fully Complementary Hybrids[a]

immobilized strand type	associating strand type	temp of kinetic exp (°C)	T_m (°C)	k_d ($\times 10^{-3}$ s^{-1})	k_a (mM^{-1} s^{-1})	K_D (M)	K_D* (M)
PNA	PNA-Lys	35	84.0	0.2	35	5.7×10^{-9}	
PNA	PNA	35	83.0	0.2	45	4.4×10^{-9}	
PNA	RNA	35	72.3	0.15	22	6.8×10^{-9}	2.6×10^{-16}
PNA	DNA	35	68.5	0.41	1.2	3.5×10^{-7}	6.5×10^{-14}
DNA	PNA	35	68.5	0.45	19	2.4×10^{-7}	6.5×10^{-14}
DNA	DNA	20	53.5	0.29	12	2.5×10^{-8}	1.5×10^{-14}

[a] K_D values are calculated from the kinetic parameters and K_D* from T_m curves at 35 (PNA•PNA, PNA•RNA, and PNA•DNA) or 20 °C (DNA•DNA).

follow quantitatively the same variation with mismatches as the PNA•DNA duplexes.

An overall fair correlation between the rate constants and the melting temperatures, T_m, was found for both the PNA•DNA and the PNA•RNA systems (Figure 4a,b). Table 1 lists the mismatches tested, the T_m values, the kinetic results obtained, and, finally, the calculated thermodynamic dissociation constants, K_D, as the ratio of the dissociation and association rate constants. The results indicate that the PNA•DNA and PNA•RNA systems behave very similarly with respect to all studied parameters upon the introduction of mismatches.

The thermally most stable duplexes (highest T_m) exhibited the slowest dissociation rates and the fastest association rates (Table 1, Figure 4a,b). The evaluated k_a and k_d values correlate well with the T_m values, and, consequently, a rather good correlation between the calculated K_D and the measured T_m of the duplexes is also obtained (Figure 5a,b). The presentation in Figure 5a,b illustrates the correlation of K_D with T_m for the investigated PNA•DNA and PNA•RNA mismatch duplexes. An approximate linearity is observed in a log K_D vs $1/T_m$ plot, indicating an empirical correlation that may be used for these systems (correlation coefficients of 0.94 for the PNA•DNA duplexes and 0.85 for the PNA•RNA duplexes). This also suggests a justification to infer the relative order of K_D values just from the measured T_m values of related systems. In full accordance with T_m measurements, the PNA•RNA duplexes (both fully matched and mismatched) showed higher association (~20-fold) and lower dissociation (~10-fold) rates and thus lower K_D (~200-fold) than the PNA•DNA duplexes.

The investigation is yet too limited in terms of variations of base sequence to allow any general conclusions about the influence of specific mismatches and sequence context.

However, we note that the PNA system appears to follow the trend of the corresponding DNA•DNA system. In particular, in our system C•X mismatches seem to be more destabilizing.

The DNA•DNA mismatch series was investigated at 20 °C instead of 35 °C due to the lower thermal stability of these duplexes (Table 2). Therefore, these results are not directly comparable with those of the PNA systems. An inverse correlation of k_d with T_m is found, while the association rate constants did not show any significant correlation with melting temperature (Figure 4c). This could be due to the very fast association ($>4 \times 10^4$ M^{-1} s^{-1}) for some of the mismatched DNA•DNA duplexes, which makes the sensorgrams difficult to analyze because the time region for association analysis then becomes very short and thus results in large statistical variations in these experiments. It is also possible that the DNA•DNA hybridization could be more sensitive to the environment (dextran) of the surface than the hybridization of DNA and RNA to the corresponding immobilized PNA (see below). This variation in association rate constant of course also affects the calculated equilibrium constant, and for some mismatch duplexes, the apparent K_D values were even lower than for the fully complementary duplex, which could hardly reflect reality and is at any rate contrasting the measured T_m. No correlation (correlation coefficient 0.51) in the log K_D vs $1/T_m$ plot was apparent (Figure 5c). In conclusion, the DNA•DNA kinetic results (Table 2) should be treated with great caution and are at any rate not essential for the main conclusions which concern the PNA complexes.

With the fully complementary PNA•PNA duplexes, a higher association rate and a lower dissociation rate were found compared to the PNA•DNA and PNA•RNA duplexes with the same sequences (Table 3). This finding agrees well with the higher T_m of the PNA•PNA complex.

Two experiments were made with the fully complementary PNA•PNA duplex either with or without a lysine residue at the C-terminal of the incoming strand. The association rate constant was found to depend somewhat on the presence of a lysine residue. It was determined to 35 mM^{-1} s^{-1} (lysine in incoming strand) and 45 mM^{-1} s^{-1} (without lysine), whereas the dissociation rate (2×10^{-4} s^{-1}) was found to be independent of the lysine (Table 3). The PNA was immobilized via biotinylation in the N-terminal, so the associating strand should hybridize with the C-terminal near the dextran. The slower association of the lysine−PNA could indicate that the lysine moiety is interfering with the dextran/streptavidin surface. This could be explained by the positively charged side chain of lysine (at pH 7) first being attracted to the negatively charged carboxylate groups of the dextran, and thereafter finding an available PNA, in contrast to the lysine-free PNA which could find an available PNA directly.

An experiment was made to investigate the effect of which strand is immobilized. For the fully complementary pentadecamer PNA•DNA duplex, both of the two possible hybridization experiments were made, i.e., with either PNA or DNA as the immobilized strand. In both cases, the dissociation rate constant was approximately 4.5×10^{-4} s^{-1}, whereas the association rate constant decreased by 1 order of magnitude in the case of PNA immobilization (from 1.9×10^4 M^{-1} s^{-1} to 1.2×10^3 M^{-1} s^{-1}) (Table 3). Since DNA is negatively charged, it should be repelled by the carboxylate groups of the dextran surface, thereby making DNA more

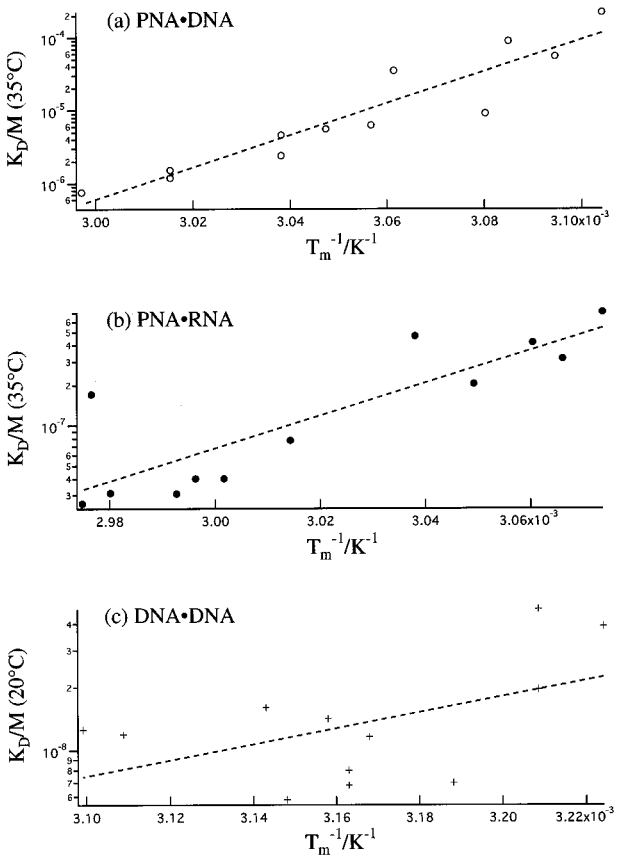

FIGURE 5: Plot of log K_D versus $1/T_m$ for the PNA•DNA (a), PNA•RNA (b), and DNA•DNA (c) mismatch duplexes. Conditions as in Figure 4. Correlation coefficients: 0.94, 0.85, and 0.51, respectively.

accessible for the incoming strand than PNA. PNA with its less hydrophilic backbone could have some affinity for the dextran, thereby complicating hybridization by making the PNA less accessible for hybridization. However, the absence of any detectable association at all to the streptavidin/dextran layer, as observed for dummy PNAs without biotin, argues against a significant PNA affinity for dextran. The variation in association rate, dependent on which strand of the duplex that is immobilized, makes it less meaningful to compare the PNA•DNA and the DNA•DNA series. However, it is appropriate to compare PNA•DNA and PNA•RNA for which the same strand (PNA) is immobilized and for which the incoming associating strands are of similar nature, thus justifying the quantitive conclusions from Table 1.

Although the association rates are not as straightforward to interpret as those of the dissociation rates, because the association mechanism at the solution/surface interface could be more complex than that of a simple association in solution, the fact that the apparent association rate constant in all cases decreases upon insertion of a mismatch indicates that it reflects not only a bulk diffusion process but also some rearrangement particular for the hybridization. This observation could indicate that the hybridization is not a simple two-state process but involves at least one precursory or outer-sphere complex, a hypothesis we intend to test by kinetic and thermodynamic techniques under free solution conditions.

The dependence on the specific environment of the strands in the present surface measurement approach makes it difficult to compare the K_D results with bulk solution data, as is apparent by comparing K_D values from the BIAcore

with K_D data obtained from melting curve analysis (Table 3). We earlier used eq 5 to estimate $\Delta H°$ and $\Delta S°$ for the same fully complementary PNA•DNA, PNA•RNA, and DNA•DNA duplexes (Egholm *et al.*, 1993). Numerical fitting of the thermodynamic parameters to the melting curves gives similar magnitudes of the thermodynamic parameters. In Table 3, corresponding K_D values are calculated from these parameters at 35 and 20 °C. Obviously, the K_D values from the melting curves are 6−7 orders of magnitude lower than those estimated here from the surface kinetic experiments. A discrepancy between K_D obtained from the melting curves and isothermal titration calorimetric measurements is also noted. For example, for a decamer PNA•DNA duplex, T_m analysis gave $K_D = 4.7 \times 10^{-11}$ M (Tomac *et al.*, 1996) while a calorimetrically determined K_D (at higher concentration) was 2.1×10^{-8} M (Lagriffoule *et al.*, 1997).

The three different methods (BIAcore, T_m analysis, calorimetry) are subject to different types of errors that might explain these variations. While the present kinetic analysis, as concluded, refers to the specific conditions of having one species attached to a surface, the T_m and calorimetric methods both apply to bulk solution conditions. However, the obviously very high thermodynamic stability of the PNA−nucleic acid complexes requires the use of correspondingly very low concentrations in order to achieve significant degrees of dissociation, at the same time as measuring sensitivity puts a lower limit to concentration. In conclusion, all K_D values determined so far for PNA−nucleic acid complexes must be considered most preliminary. We are currently considering alternative, more sensitive detection techniques for their determination in the limit of extremely dilute bulk solution.

CONCLUSIONS

The introduction of a single mismatch at the center of pentadecamer PNA•DNA and PNA•RNA duplexes gives rise to changes in the association (hybridization) and dissociation kinetics that can be conveniently assessed using the BIAcore technique with a surface-immobilized (static) PNA oligomer. The following conclusions can be made for the PNA•DNA and PNA•RNA hybridizations:

(1) Overall decreased association and increased dissociation rate constants (K_D^{-1}) correlate generally with decreased melting temperatures (T_m).

(2) A higher thermal stability was generally found for PNA•RNA duplexes compared to PNA•DNA duplexes.

(3) The observation that also the effective association constants are affected by the choice of nucleobase sequence indicates that the rate-limiting step involves more than a bulk diffusion process.

ACKNOWLEDGMENT

We are grateful to Drs. Petter Björgqvist and Johanna Deinum, Astra Hässle Co., for generously allowing us to use their BIAcore equipment. We also thank Mrs. Annette W. Jørgensen for skillful technical assistance in the T_m measurements.

REFERENCES

Bonham, M. A., Brown, S., Boyd, A. L., Brown, P. H., Bruckenstein, D. A., Hanvey, J. C., Thomson, S. A., Pipe, A., Hassman, F., Bisi, J. E., Froehler, B. C., Matteucci, M. D., Wagner, R. W., Noble, S. A., & Babiss, L. E. (1995) *Nucleic Acids Res. 23*, 1197−1203.

Christensen, L., Fitzpatrick, R., Gildea, B., Petersen, K. H., Hansen, H. F., Koch, T., Egholm, M., Buchardt, O., Nielsen, P. E., Coull, J., & Berg, R. H. (1995) *J. Peptide Sci. 3*, 175−183.

Demidov, V., Frank-Kamenetskii, M. D., Egholm, M., Buchardt, O., & Nielsen, P. E. (1993) *Nucleic Acids Res. 21*, 2103−2107.

Demidov, V., Potaman, V. N., Frank-Kamenetskii, M. D., Buchardt, O., Egholm, M., & Nielsen, P. E. (1994) *Biochem. Pharmacol. 48*, 1309−1313.

Demidov, V. V., Cherny, D., Kurakin, A. V., Yanilovich, M. V., Malkov, V. A., Frank-Kamenetskii, M. D., Sönnichsen, S. H., & Nielsen, P. E. (1995) *Nucleic Acids Res. 22*, 5218−5222.

Dueholm, K. L., Egholm, M., Behrens, C., Christensen, L., Hansen, H. F., Vulpius, T., Petersen, K., Berg, R. H., Nielsen, P. E., & Buchardt, O. (1994) *J. Org. Chem. 59*, 5767−5773.

Egholm, M., Buchardt, O., Christensen, L., Behrens, C., Freier, S. M., Driver, D. A., Berg, R. H., Kim, S. K., Norden, B., & Nielsen, P. E. (1993) *Nature 365*, 556−568.

Egholm, M., Christensen, L., Dueholm, K., Buchardt, O., Coull, J., & Nielsen, P. E. (1995) *Nucleic Acids Res. 23*, 217−222.

Fägerstam, L. G., & Karlsson, R. (1993) *Immunochemistry* (van Oss & van Regenmortel, Eds.) pp 949−970, Marcel Dekker Inc., New York.

Gotoh, Y. M. H., Shinohara, Y., Shimizu, T., & Mizuho, M. (1995) *DNA Res. 2*, 285−293.

Hanvey, J. C., Peffer, N. C., Bisi, J. E., Thomson, S. A., Cadilla, R., Josey, J. A., Ricca, D. J., Hassman, C. F., Bonham, M. A., Au, K. G., Carter, S. G., Bruckenstein, D. A., Boyd, A. L., Noble, S. A., & Babiss, L. E. (1992) *Science 258*, 1481−1485.

Jönsson, U. (1991) *BioTechniques 11*, 620−627.

Knudsen, H., & Nielsen, P. E. (1996) *Nucleic Acids Res. 24*, 494−500.

Lagriffoule, P., Wittung, P., Eriksson, M., Kilså Jensen, K., Nordén, B., Buchardt, O., & Nielsen, P. E. (1997) *Chem.—Eur. J.* (submitted for publication).

Malmqvist, M. (1993) *Immunotechnology Colloqium at 22nd FEBS Letters Meeting Dublin 1992* (Gosling, J. P., & Reen, D., Eds.) pp 61−75, Portland Press, Colchester, U.K.

Malmqvist, M., & Granzow, R. (1994) *Methods: Companion Methods Enzymol. 6*, 95−98.

Marky, L. A., & Breslauer, K. J. (1987) *Biopolymers 26*, 1601−1620.

Nielsen, P. E., Egholm, M., Berg, R. H., & Buchardt, O. (1991) *Science 254*, 1497−1500.

Nielsen, P. E., Egholm, M., & Buchardt, O. (1994a) *Bioconjugate Chem. 5*, 3−7.

Nielsen, P. E., Egholm, M., & Buchardt, O. (1994b) *Gene 149*, 139−145.

Nielsen, P. E., & Ørum, H. (1995) *Molecular Biology: Current Innovations and Future Trends* (Griffin, H., Ed.) pp 73−86, Horizon Scientific Press, U.K.

Nilsson, P., Persson, B., Uhlén, M., & Nygren, P.-Å. (1995) *Anal. Biochem. 224*, 400−408.

Ørum, H., Nielsen, P. E., Egholm, M., Berg, R. H., Buchardt, O., & Stanley, C. (1993) *Nucleic Acids Res. 21*, 5332−5336.

Ørum, H., Jørgensen, M., Koch, T., Nielsen, P. E., Larsson, C., & Stanley, C. (1995) *BioTechniques 19*, 472−480.

O'Shannessy, D. J., Brigham-Burke, M., Soneson, K. K., & Hensley, P. (1993) *Anal. Biochem. 212*, 457−468.

Tomac, S., Sarkar, M., Ratilainen, T., Wittung, P., Nielsen, P. E., Nordén, B., & Gräslund, A. (1996) *J. Am. Chem. Soc. 118*, 5544−5552.

Veselkov, A. G., Demidov, V., Nielsen, P. E., & Frank-Kamenetskii, M. D. (1996) *Nature 379*, 214.

Wood, S. J. (1993) *Microchem. J. 47*, 330−337.

BI9627525